

IV. SPECIAL CASE: POISSON PROCEDURES

For certain stochastic processes it is possible to determine the fractional area coverage from measurements along a line without any *a priori* knowledge of the process. Here such a possibility is given for a Poisson line process like the one used above as a model of leads.

For a Poisson process the area fraction is related to the intensity¹ τ of the process and the mean "area" of the objects ζ :

$$p' = \Pr[O \text{ is covered}] = 1 - e^{-\tau\zeta} \quad (6)$$

where O is an arbitrary origin. The area measure corresponds in units to the intensity measure; e.g., for leads the intensity is the number of points per unit distance and ζ is mean lead width.

The area fraction can be now estimated from lineal measurements through the use of the line (lead) thickness (width) distribution. The area term in (6) is the overall mean line thickness, W , defined as

$$W = \pi^{-1} \int_0^\pi w(\theta) d\theta$$

where $w(\theta)$ is the mean thickness of lines with orientation θ ($0 \leq \theta \leq \pi$) [4]. This applies to lines oriented isotropically; i.e., with a uniform distribution such that $f_\Theta(\theta) = \pi^{-1}$ where f_Θ is the probability density function for line (lead) orientations. For anisotropic thick lines then

$$W = \int_0^\pi w(\theta) dF_\Theta(\theta)$$

where $dF_\Theta(\theta) = f_\Theta(\theta)d\theta$, and F_Θ is the cumulative distribution function for orientations. A method for determining the actual lead width distribution, and hence W , from the width distribution measured along a transect has been presented in [3].

As an example of the use of (6), the lead network in Fig. 1(b) was generated with $\tau = 1/3$ (3-km mean spacing) and $W = 0.2$ km. This gives a p' estimate using (6) of 0.064 compared to the value of 0.067 reported in Table II. The discrepancy is a function of the image creation and thresholding process, where all leads must fill an entire pixel.

In practice the intensity of the process is not known. For leads modeled as a Poisson line process an estimate of τ can be obtained from the transect data, where the points of intersection of the transect with leads constitute a Poisson process of intensity $2\tau/\pi$. The accuracy of this estimate depends on the size of the region over which the measurements are made. For Fig. 1(b) estimates of τ range from 0.19 to upwards of 0.45 which results in an estimate of p' in the range of 0.037 to 0.086. There is, of course, some variability in the estimate of W as well, which is discussed in [3].

V. SUMMARY

A general method has been presented that allows for the assessment of potential errors in estimating the fractional coverage of geophysical variables from measurements along a line. Potential applications include the analysis of field data from aircraft, ships, and submarines as well as data collected on along ground transect by field personnel. For image processing the primary use of transect measurements is in the sampling of very large data sets. By application to fields of clouds and sea ice fractures it was shown how the variance of the estimate of area fraction depends on the spatial structure and the

¹The intensity of a stochastic process is commonly called the density of the process. The former term is used here in order to avoid confusion with the concept of probability density.

number and length of transects in the sample. With a single, short transect the estimated fractional coverage has a large variance. With large samples the sampling distribution of sample proportions tends towards normal with a mean equal to the population or true mean, so that confidence interval estimates and hypothesis tests are possible.

The shortcoming of the approach is that the autocovariance function must be known. If, however, it is assumed that some basic autocovariance structure exists for different cloud types, sea ice leads, etc., possibly as a function of the time of year and/or geographic location, the general lineal method is a useful tool. Even if such *a priori* knowledge of the geophysical field is not available, the method allows for the assessment of sampling errors and the design of sampling strategies in a general sense. In cases where the spatial structure of a geophysical variable can be described by a particular stochastic process such as a Poisson process, other methods of estimating the area coverage may be available.

ACKNOWLEDGMENT

The author thanks H. Maybee and S. Peckham, and D. Rothrock for useful discussions.

REFERENCES

- [1] D. Stoyan, W. S. Kendall, and J. Mecke, *Stochastic Geometry and its Applications*. New York: Wiley, 1989.
- [2] D. A. Rothrock and A. S. Thorndike, "Measuring the sea ice floe size distribution," *J. Geophys. Res.*, vol. 89, no. C4, pp. 6477-6486, 1984.
- [3] J. Key and S. Peckham, "Probable errors in width distributions of sea ice leads measured along a transect," *J. Geophys. Res.*, vol. 96, no. C10, pp. 18417-18423, 1991.
- [4] R. E. Miles, "Random polygons determined by random lines in a plane," *Proc. Nat. Acad. Sci.*, vol. 52, pp. 901-907, 1964.

LAI Inversion Using a Back-Propagation Neural Network Trained with a Multiple Scattering Model

James A. Smith

Abstract—Standard regression methods applied to canopies within a single homogeneous soil type yield good results for estimating leaf area index (LAI) but perform unacceptably when applied across soil boundaries. In contrast, the neural network reported here generally yielded absolute percentage errors of < 30%. The network was applied, without retraining, to a Landsat TM.

1. INTRODUCTION

Current and projected satellite sensor systems, e.g., the Moderate Resolution Imaging Spectrometer (MODIS) [1], are able to obtain global and repetitive observations at high temporal sampling rates and many studies have demonstrated the utility of vegetation indices at continental scales for estimating photosynthetic processes and leaf area index (LAI) in plant communities [2]. Others, however, have

Manuscript received May 17, 1993.

The author is with the NASA Goddard Space Flight Center, Greenbelt, MD 20771.

IEEE Log Number 9212140.

indicated the limitations of vegetation indices for LAI and absorbed photosynthetically active radiation (APAR) assessment [3].

Regression relationships have long been used to relate leaf area index and other vegetation characteristics to remote sensing observables [4]. Unfortunately, these relationships are known to vary widely as a function of soil color [5] and atmospheric effects [6]. To attempt to circumvent these difficulties several investigators have tried direct inversion of canopy reflectance models [7] or indirect inversion by employing minimization methods with respect to LAI and merit functions constructed from differences between measured and predicted reflectances [8], [9]. While promising, these methods are strongly dependent upon a good initial guess of the desired parameter and, for the most part, have not been applied to broad scale satellite data analysis.

Recently, some new approaches to this problem have been developed by combining physically based models and measurements with either artificial intelligence concepts [10] or neural computing techniques [11]. Tsang *et al.* [12] used a neural network trained with a multiple scattering model to infer snow parameters from passive microwave remote sensing measurements.

The objective of this study is to investigate the use of a back-propagation neural network, trained with a multiple scattering model, for improved leaf-area-index estimation, particularly for sparse canopies overlying varying soil backgrounds, where standard techniques have difficulty. The selection of neural network operating parameters is explored using simulation analysis. Genetic algorithm inversion analysis of the trained neural network is also performed to gain insight into the network operating characteristics. The learned network weights are then applied to sample satellite Thematic Mapper data for an agriculture/forestry study site.

II. STUDY AREA

The Mogi-Guaçu study area is located between 22° 05' to 22° 20' South latitude and 47° 00' to 47° 15' West longitude in the São Paulo State and is representative of pine and eucalyptus plantations common to that region. This site includes the Campininha Pine Experimental Station of the Forestry Institute of the state of São Paulo (IFSP) and the Santa Terezinha Eucalyptus Plantation of the Champion Cellulose and Paper Company (CCP). The major *Pinus* species in Campininha are *Pinus elliottii* and *Pinus taeda*. Other species, such as *Pinus caribaea*, *Pinus bahamensis*, *Pinus oocarpa*, and *Pinus palustris*, are also planted in small amounts. The prominent Eucalyptus species in Santa Terezinha are *Eucalyptus alba* and *Eucalyptus saligna*.

Field data and forest cover maps were provided by IFSP and CCP and may be grouped into four forest classes based on species or age. These classes refer to *Pinus elliottii*, *Pinus* species other than *Pinus elliottii*, Eucalyptus spp. from eight months to two years, and Eucalyptus spp. over two years. The pine plantation is composed of tree stands varying from 10 to 30 years and the eucalyptus plantation from one to less than seven years.

III. THEORY

A. Multiple Scattering Models

A relatively simple reflectance model was employed since we are looking at the application of the technique to large-scale satellite data analysis where the availability of scene-dependent parameters necessary to drive such models is limited. Specifically, we utilize the simple two-stream Kubelka Munk model [13]. This is the model also used by Price [14] in his analysis of AVHRR data and requires minimal input.

The two-stream approximation for upwelling flux, I , and downwelling flux, J , is given by

$$\frac{dI}{dn} = (k + s)I + J \text{ and } \frac{dJ}{dn} = -sI + (k + s)J.$$

The leaf scattering coefficient, s , and leaf absorption coefficient, k , are determined from measured individual leaf reflectance and transmittance measurements. The canopy depth dimension is taken as the cumulative leaf area index, n , measured downward from the top of the canopy. Multiple scattering of radiant flux within the canopy is governed by the indicated coupled differential equations subject to the boundary conditions

$$J(LAI) = \rho_g * I(LAI) \text{ and } I(0) = 1.$$

These equations can then be solved for canopy reflectance, ρ_c , as a function of leaf area index (LAI), background soil reflectance, ρ_g , and leaf optical scattering properties, k and s . All quantities vary with wavelength except LAI (see the equation at the bottom of this page).

B. Back-Propagation Neural Network Technique

A multilayer, feedforward artificial neural network (ANN) consists of an input layer, one or more hidden layers, and an output layer of fully interconnected neurons. Each neuron computation unit produces an output based on some function, usually a sigmoid function, of a linear combination of outputs from neurons in a previous layer. There are two general steps in the training of a back-propagation ANN. These consist first of a feedforward iteration to calculate the output of the network, as a function of the interconnection weights, based on training input values presented to the input layer. This is then followed by a back-propagation learning rule, which is an iterative gradient descent algorithm designed to minimize the mean squared error between network predicted outputs and training set values. For a three-layer network, which was employed in this study, the procedure is as follows [15]:

The net input to a hidden neurode, i_j , is the weighted sum of the outputs from the input layer, o_i , i.e.,

$$i_j = \sum_i w_{ji} o_i$$

where w_{ji} is the interconnection weight between input neurode i and hidden neurode j . The output from a hidden neurode, j , is given by

$$o_j = \frac{1}{1 + e^{-i_j}}.$$

$$\rho_c = \frac{(1 - b^2)(e^{aLAI} - e^{-aLAI}) - \rho_g[(1 - b^2)e^{aLAI} - (1 + b)^2e^{-aLAI}]}{(1 + b)^2e^{aLAI} - (1 - b)^2e^{-aLAI} - \rho_g(1 - b^2)(e^{aLAI} - e^{-aLAI})}$$

where

$$a = \sqrt{k(k + 2s)} \text{ and } b = \sqrt{k/(k + 2s)}.$$

The net input to an output neurode, i_l from the hidden layer is similarly given as a weighted sum over $w_{lj}o_j$ and the output from an output node, o_l is the sigmoid function of i_l . Training by gradient descent leads to the following iterative expressions for weight updating:

$$w_{lj} = w_{lj} + \eta \delta_l o_j + \alpha \Delta w_{lj}$$

and

$$w_{ji} = w_{ji} + \eta \delta_j o_i + \alpha \Delta w_{ji}$$

where

$$\delta_l = (t_l - o_l) o_l (1 - o_l)$$

and

$$\delta_j = o_j (1 - o_j) \sum w_{lj} \delta_l$$

t_l is the desired target result for output neurode, l , η , the learning rate, and α a damping or momentum term.

The basic strategy for the inversion of surface parameters, e.g., LAI, from optical remote sensing data using a back-propagation ANN is thus to present a set of training data, $\{o_i, t_i\}$, to the network where o_i represents either spectral reflectance channels directly or some combination of these channels and t_i represents the desired surface parameter, here LAI.

There are, however, a number of practicalities involved in the application of an ANN to the parameter inversion problem. The neural network parameters, e.g., the number of iterations required for convergence, the appropriate number of hidden nodes and layers, learning rate and momentum term must all be investigated. The role of pre- and postprocessing transformations to enhance learning and robustness are sometimes key to system performance. Finally, once a network has been trained, the interpretation of system performance and a physical understanding of the network categorization is important to understand its extrapolation capabilities under different scene conditions. In this latter regard, we have found it useful to apply genetic algorithms to the learned network weights to visualize the network partitioning of the input feature space [16].

IV. METHOD

The generation of training and test sample data sets was performed using the simple two-stream, radiative transfer model discussed earlier to predict canopy reflectance as a function of soil reflectance, LAI, and leaf optical properties. Attention was focused on sparse canopies, $LAI < 1.0$, and two soil backgrounds. These data were then used in multiple regression analyses to establish the need for an alternate solution, e.g., ANN's, and for benchmark comparisons. The neural network was trained on one sample of canopy reflectance data generated using one soil type and tested on a second, independent canopy reflectance data set generated using a second soil type. The ability of the network solution to generalize to new data was thus evaluated. The multiple regression solutions were similarly developed and tested for these cases. Experimental data required to run the scattering model to train and test the neural network were obtained from an intensive sensor fusion field experiment in Maine during the summer of 1990 [17].

A. The Direct Problem—Generation of Training and Test Samples

Measured leaf reflectance and transmittance data as well as soil reflectance data were obtained from the Maine sensor fusion field experiment. Three wavelengths were chosen for analysis corresponding to the green reflectance peak at $0.55 \mu\text{m}$ (TM2), the red chlorophyll absorption band at $0.67 \mu\text{m}$ (TM3) and the infrared plateau at $0.80 \mu\text{m}$ (TM4).

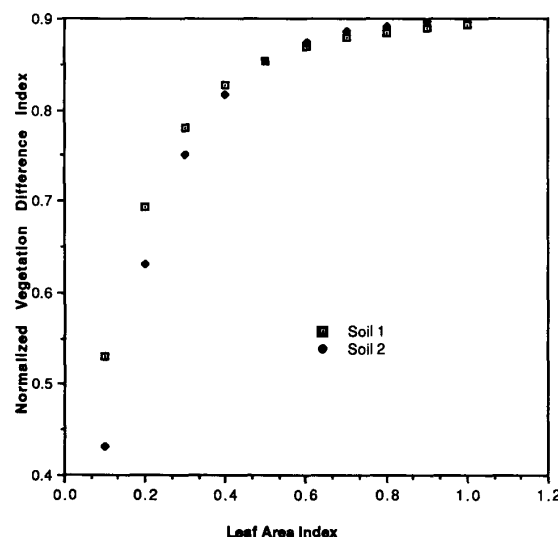


Fig. 1. Normalized difference vegetation index versus leaf area index for two soil types as calculated from simulated reflectance data.

μm (TM4). These latter two wavelengths were also required to calculate the normalized difference vegetation index (NDVI). The measured soil reflectance values corresponded to a medium dark soil. A second set of assumed soil reflectance factors was calculated from the measured data using the method of Baret and Guyot [3] and corresponded to a medium bright soil.

Leaf area index was varied from 0.1 to 1.0 in steps of 0.1 corresponding to sparse canopies. Thus 10 canopy reflectance measurements were obtained for each of two soil types at each of three wavelengths. The 10 triplets of canopy reflectance values corresponding to the ten simulated leaf area indices for soil type 1 were treated as the training set. Similarly, the 10 triplets of canopy reflectance values corresponding to the same ten leaf area indices but for soil type 2 were treated as the testing set.

B. Multiple Regression Analysis

Straightforward multiple regression of leaf area index, LAI, against reflectance at $0.55 \mu\text{m}$, ρ_{55} , reflectance at $0.67 \mu\text{m}$, ρ_{67} and at $0.8 \mu\text{m}$, ρ_{80} , verified that while a good relationship could be developed for measurements obtained over only soil type 1 or only over soil type 2, neither relationship could be applied to data of the other soil type. Fig. 1 shows reduction in the variation of NDVI for the two soil types at higher LAI, but significant differences are still evident for $LAI < 0.5$.

After some experimentation the following multiple regressions were obtained between LAI versus ρ_{55} and NDVI. The R -squared values are included only for reference. The results section gives the application of these equations to calculate the absolute percent error in predicted LAI for each LAI between 0.1 and 1.0.

Using Soil 1 data only:

$$LAI = -5.85 + 80.1\rho_{55} - 6.98NDVI \quad R\text{-squared} = 94\%$$

Using Soil 2 data only:

$$LAI = 30.7 - 148\rho_{55} - 6.12NDVI \quad R\text{-squared} = 98\%$$

Using both Soil 1 and Soil 2 data:

$$LAI = -1.34 + 2.58\rho_{55} + 1.88NDVI \quad R\text{-squared} = 71\%.$$

For a strict comparison between the use of multiple regression versus the neural network approach, only the equation for Soil 1 should be applied to the Soil 2 data (or vice versa). However, because of the large (off-scale) errors so obtained, the third regression equation was also obtained and applied to Soil 2 data to show comparisons within the same scale as the neural network.

The results for regression analysis given in Section V clearly indicate the need for other approaches.

C. Neural Network Analysis

A considerable amount of computer time and personnel resources are required in order to hone in on an optimum ANN solution. A number of runs are required to fully explore the effect of the number of hidden nodes, number of iterations, learning rate, and momentum term on overall performance. For each exploration, replication with a set of random initial weight matrices would be desirable and appropriate averaging of the results performed.

However, within the constraints of this analysis a good solution that would be both feasible and demonstrably better than, e.g., the multiple regression method, was sought. Ground estimation techniques of LAI using destructive sampling methods rarely yield an absolute percent error estimate of better than 30% and this was taken as an approximate definition of a good solution.

A pragmatic approach was taken. Based on the multiple regression analyses described earlier, the input data to the neural network was taken to be the reflectance at $0.55 \mu\text{m}$, ρ_{55} , and the normalized vegetation index, NDVI. Both variables are bounded by 0 and 1.0. The desired output of the network is the LAI estimate. A feedforward network using 1 hidden layer with a 2 [input nodes] \times N [hidden nodes] \times 1 [output node] was selected. The number of hidden nodes was initially selected to be the "number of input nodes + number of output nodes + a few" or 7. The learning rate was selected to be 0.15 and was not varied. The momentum value was initially selected to be 0.5, however, a broad exploration quickly established that the network was not sensitive to the momentum term and a value of 0.9 was adequate.

Attention was focused on the effect of random initial weights, the number of iterations, and the possible increase in the number of hidden nodes to 11. The number of iterations studied was 2000, 6000, and 10 000. Three runs were made for each iteration test corresponding to different random initial weight matrices. The network was first trained on the reflectance data for soil type 1 for the specified number of iterations and then tested with the reflectance data for soil type 2. The absolute percent error for each LAI within the range of 0.1 to 1.0 was summarized and compared, particularly for low LAI values. The total normalized rms error for each run was also compared but this was not as instructive as the overall pattern of LAI estimation errors.

It was evident that the network was beginning to be overtrained at 10 000 iterations indicating that a reasonable bracket of iteration count had been explored. Variations of a few percent in absolute LAI error resulting from different random initial weight matrices were not deemed significant. The total rms errors were also comparable between runs for a given iteration count. Sample runs with 11 hidden nodes showed either comparable or decreased performance.

V. RESULTS

A. Regression Results

Applying the Soil 1 regression equation to Soil 2 data yields absolute percent errors of 6062, 1995, 844, 4171, 223, 68, 34, 12, and 8 corresponding to LAI of 0.1, 0.2, 0.3, 0.4, 0.5, 0.6, 0.7, 0.8, 0.9, and 1.0. Similarly, the application of the regression equation

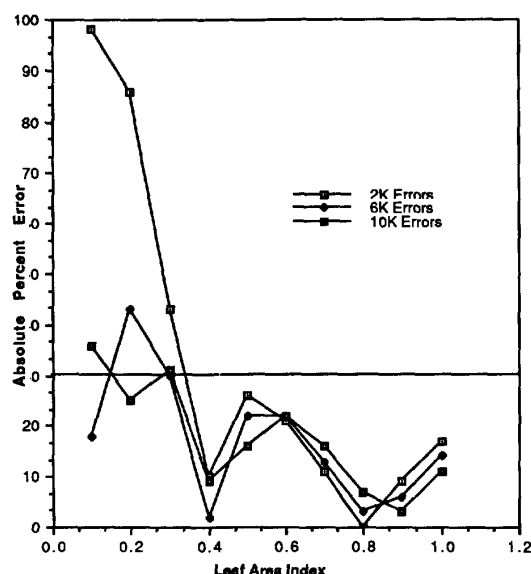


Fig. 2. Neural network error performance as a function of number of training iterations.

developed over both Soil 1 and Soil 2 data applied to Soil 2 data only yields the following corresponding values: 145, 54, 73, 59, 40, 22, 7, 5, 15, and 23.

B. Neural Network Results and Interpretation

Since comparable results were obtained with all three random initial weight matrices, one was selected arbitrarily. A plot of the absolute percent error variation with LAI as a function of number of iterations is shown in Fig. 2. The horizontal 30% absolute error line taken as an indicator of a good solution has also been drawn. The matrix trained with 6000 iterations and using a 2 by 7 by 1 architecture was deemed to satisfy the criteria of a good solution, generally less than 30% absolute percent error. The technique also shows dramatic improvement over the multiple regression results given above for these conditions.

In order to understand how the trained neural network estimated LAI, a genetic algorithm was employed to do an inverse mapping of the neural network decision surfaces for LAI [16]. Random populations of two genes, corresponding to values of NDVI and ρ_{55} , respectively, were presented to the algorithm. The genetic algorithm samples the decision space by generating new populations of genes, LAI and ρ_{55} values, based on fitness value calculations subject to crossover and mutation. Differences between the neural network output and a desired decision surface threshold corresponded to the fitness function. Fig. 3 shows the family of decision surfaces corresponding to LAI values of 0.1 to 1.0 in steps of 0.1. The training and test simulation points for the two soil backgrounds are also plotted on the same graph. The network is generally able to separate the range of LAI values for both training and test samples but it requires a family of linear decision surfaces with nonlinear separation.

Finally, the trained network was applied to digital satellite data for Mogi-Guaçu. TM data from path 220/row 75, corresponding to the April 15, 1989 overpass of the area, were used. No atmospheric corrections were applied, but the data were preprocessed to effective reflectance at the top of the atmosphere [18]. The derived LAI distribution is shown in Fig. 4. Dark grey levels correspond to low LAI with brighter values corresponding to high LAI. The bare fields, field

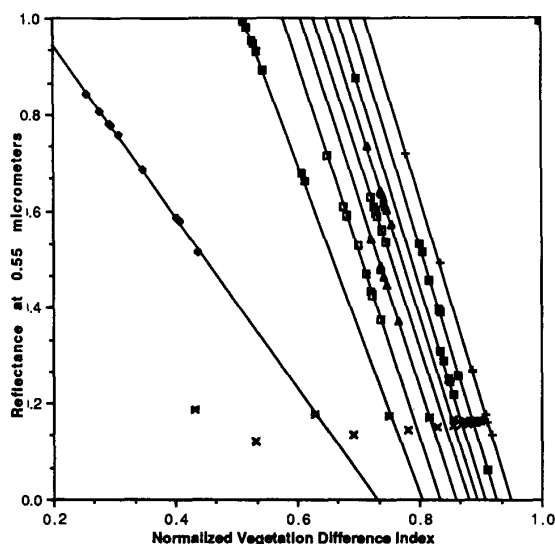


Fig. 3. Genetic inverse mapping of neural network feature space. Straight lines (from left to right) correspond to decision boundaries for successively increasing values of LAI.



Fig. 4. Neural network leaf area index image for 1989 Thematic Mapper scene of Mogi-Guaçu. (North is to the left.)

and road boundaries, and relative mapping of new growth Eucalyptus with high LAI and pine plantation with lower LAI have been correctly differentiated.

VI. SUMMARY

For the simulation analyses performed, the neural network was able to map LAI from reflectance data with accuracies comparable to that obtained from ground observations and proved more robust than standard regression techniques when applied to varying soil backgrounds. Initial application of the network to satellite data, even without retraining, provided good qualitative comparisons with available ground control information.

While the technique appears promising, further exploration under a greater variety of soil reflectance backgrounds and solar illumination and viewing geometries is warranted. A wider variety of training and test samples for these varying conditions need to be generated in order to understand the limits of the network approach. In order to

understand these more complex cases, other reflectance models which incorporate full bidirectional properties may need to be employed. Quantitative comparisons of satellite-derived LAI with field data is also required for calibration. Finally, it should be noted that other neural network architectures may also lend themselves to the class of problems described here.

ACKNOWLEDGMENT

The author expresses his appreciation to Dr. Shimabukuro from the Instituto Nacional de Pesquisas Espaciais—INPE, São Paulo, Brazil, for providing the TM satellite data for Mogi-Guaçu and helpful discussions in the interpretation of the neural network results for that area.

REFERENCES

- [1] V. V. Salomonson, W. L. Barnes, P. W. Maymon, H. Montgomery, and H. Ostrow, "MODIS: Advanced facility instrument for studies of the Earth as a system," *IEEE Trans. Geosci. Remote Sensing*, vol. GE-27, pp. 45–133, 1989.
- [2] S. N. Goward, C. J. Tucker, and D. G. Dye, "North American vegetation patterns observed with the nimbus-7 advanced very high resolution radiometer," *Vegetatio*, vol. 64, pp. 3–14, 1985.
- [3] F. Baret and G. Guyot, "Potentials and limits of vegetation indices for LAI and APAR assessment," *Remote Sensing Environ.*, vol. 35, pp. 161–173, 1991.
- [4] D. L. Peterson, M. A. Spanner, S. W. Running, and K. B. Teuber, "Relationship of thematic mapper simulator data to leaf area index of temperate coniferous forests," *Remote Sensing Environ.*, vol. 22, pp. 3223–341, 1987.
- [5] A. R. Huete, "A soil-adjusted vegetation index (SAVI)," *Remote Sensing Environ.*, vol. 25, pp. 295–309, 1988.
- [6] Y. J. Kaufman and D. Tanré, "Atmospherically resistant vegetation index (ARVI) for EOS-MODIS," *IEEE Trans. Geosci. Remote Sensing*, vol. GE-30, pp. 261–270, 1992.
- [7] J. Franklin and A. H. Strahler, "Invertible canopy reflectance model of vegetation structure in semiarid woodland," *IEEE Trans. Geosci. Remote Sensing*, vol. GE-26, pp. 809–825, 1988.
- [8] N. S. Goel and R. L. Thompson, "Inversion of vegetation canopy reflectance models for agronomic variables. V. Estimation of LAI and average leaf angle using measured canopy reflectances," *Remote Sensing Environ.*, vol. 16, pp. 69–85, 1984.
- [9] A. Kuusk, "Determination of vegetation canopy parameters from optical measurements," *Remote Sensing Environ.*, vol. 37, pp. 207–218, 1991.
- [10] D. S. Kimes and P. R. Harrison, "A knowledge-based expert system for inferring vegetation characteristics," *Int. J. Remote Sensing*, vol. 12, pp. 1987–2020, 1991.
- [11] A. Ishimaru, R. J. Marks, L. Tsang, C. M. Lam, and D. C. Park, "Particle size distribution determination using optical sensing and neural networks," *Opt. Lett.*, vol. 15, no. 21, pp. 1221–1223, 1990.
- [12] L. Tsang, Z. Chen, Oh Seho, R. J. Marks II, and A. T. C. Chang, "Inversion of snow parameters from passive microwave remote sensing measurements by a neural network trained with a multiple scattering model," *IEEE Trans. Geosci. Remote Sensing*, vol. GE-30, pp. 1015–1024, 1992.
- [13] W. A. Allen and A. J. Richardson, "Interaction of light with a plant canopy," *J. Opt. Soc. Amer.*, vol. 58, no. 8, pp. 1023–1028, 1968.
- [14] J. C. Price, "Estimating leaf area index from remotely sensed data," in *Proc. IGARSS '92*, Houston, TX, May 26–29, 1992, pp. 1500–1502.
- [15] R. C. Eberhart, and R. W. Dobbins, Eds., *Neural Network P.C. Tools*. New York: Academic, 1990.
- [16] L. Davis, Ed., *Handbook of Genetic Algorithms*. New York: Van Nostrand Reinhold, 1991.
- [17] J. A. Smith, K. J. Ranson, D. L. Williams, E. R. Levine, S. M. Goltz, and R. S. Katz, "Sensor-fusion field experiment in forest ecosystem dynamics," *Proc. SPIE Int. Soc. Opt. Eng.*, vol. 1300, pp. 117–132, 1990.
- [18] B. L. Markham and J. L. Barker, "Landsat MSS and TM postcalibration dynamic ranges exoatmospheric reflectances and at-satellite temperatures," EOSAT, Lanham, MD, Landsat Tech. Notes, Landsat User Notes, 1986.